J Solid State Electrochem (2018) 22:169–180
DOI 10.1007/s10008-017-3731-z

ORIGINAL PAPER

Coupled electrochemical-chemical procedure used in construction of molecularly imprinted polymer-based electrode: a highly sensitive impedimetric melamine sensor

Mojtaba Shamsipur[1] · **Nozar Moradi**[1] · **Afshin Pashabadi**[1]

Received: 11 July 2017 / Revised: 9 August 2017 / Accepted: 11 August 2017 / Published online: 25 August 2017

Abstract A novel molecularly imprinted sensor was fabricated and used for the impedimetric detection of melamine. Considering the identity of polymeric film and the pK_a of a melamine template, an effective procedure was established to construct the MIP-based melamine sensor. The proposed method is based on the electropolymerization of pyrrole (Py) in the presence of melamine on the electrochemically reduced graphene oxide modified glassy carbon electrode (ERGO/GCE), followed by treatment with the solution of 1% H_2O_2 in alkaline water/CH_3CN-mixed solvents. The surface morphology and the electrical feature of molecularly imprinted polymer (MIP) were characterized by scanning electron microscopy (SEM), Fourier transformation infrared spectroscopy (FTIR), cyclic voltammetry (CV), and electrochemical impedance spectroscopy (EIS). The EIS was also utilized to transduce the change of charge transfer resistance (R_{ct}) at the interface of polymer film-electrolyte, after subsequent incubation of electrode in the solution containing different concentrations of analyte, and consequently, a linear response was obtained over the range of 4.0 to 240 nM with a detection limit of 0.83 nM (S/N = 3). The effect of possible interferences on the response of sensor was studied, and the results confirmed the good selectivity of the proposed device for melamine assay. The MIP sensor was successfully applied to determine melamine in a multiple concentration-spiked milk sample.

Keywords Impedimetric sensor · Molecularly imprinted polymer · Electropolymerization · Melamine · Pyrrole

✉ Mojtaba Shamsipur
mshamsipur@yahoo.com

[1] Department of Chemistry, Razi University, Kermanshah, Iran

Introduction

Melamine ($C_3H_6N_6$), a kind of triazine analogue with three amino groups, is an industrial chemical used in the production of melamine-formaldehyde resins [1, 2]. It contains 66 wt% of nitrogen, and has been used as a filler for protein-rich diets by unethical manufacturers. This fact was mirrored in the pet food incident in early 2007, and the milk products disgrace recently when melamine was added to raw materials to get high protein contents [3]. It has low oral acute toxicity, but the chronic administration of high concentrations can induce renal pathology and even death, especially in babies and children [4]. Melamine in combination with cyanuric acid is able to form insoluble melamine cyanurate crystals in the kidney, which causes renal failure.

This situation prompted the US Food and Drug Administration (FDA), the European community, and other countries to establish the criteria of maximum residue limits for melamine in various food products. The standard limits of 1 ppm for melamine in infant formula and 2.5 ppm in other milk products have been introduced by many countries [5]. Consequently, a sensitive and reliable method is urgently needed to monitor it in food and, particularly, in dairy products for children.

Conventionally, determination of melamine in various real samples has been performed using gas chromatography; high-performance liquid chromatography [6, 7]; infrared [8], mass [9], and nuclear magnetic resonance spectroscopy [10]; electrophoresis [11]; and chemiluminescence detection [12, 13]. Unfortunately, the current methods, although mostly accurate and sensitive, are difficult to be implemented because of complicated instruments and time-consuming sample pretreatments [5, 12, 14]. Recently, some works have also been developed for the analysis of melamine based on optical techniques [15, 16] and electrochemical techniques [17–20]. Some

reports on application of molecularly imprinted polymers in construction of a variety of electrochemical sensors were recently published [21–24]. Several methods for preparation of molecular imprinting polymers (MIPs) have been reported frequently based on soft lithography technique [25], molecular self-assembled approach [26], and electropolymerization [27].

The electropolymerization methods have some attractive features including easy adherence of the polymeric films on the surface of electrodes and the ability to control thickness of the films under different deposition conditions [28]. The materials containing electroactive moieties such as pyrrole (Py), thiophene, ethylenedioxythiophene, aniline, *ortho*-phenylenediamine, and phenolic-based compounds have been extensively used to establish chemosensors based on the concept of molecular imprinting [29]. Among these monomers, Py and its derivatives are of particular interest, owing to their high conductivity, availability of the initial monomers, stability in the oxidized state, and interesting redox properties. Various chemical and electrochemical approaches extended for synthesis of PPy [30–32], in which the polymer chains are formed during the polymerization of Py [31]. In some works, PPy undergoes overoxidation at positive potentials, an undesirable degradation process, causing loss of film conductivity because of ejection of dopant and formation of oxygen-containing groups such as carboxyl and carbonyl at the pyrrole units [33]. In contrast, chemical oxidation of PPy films leads to the formation of polarons, introduced as charge associated with the lattice distortion, which increases conductivity of electroactive PPy-based films [34].

It is obvious that the sensitivity of the MIP-based sensors is directly dependent on the number of effective imprinted sites embedded in the sensing interface. In order to increase this feature, graphene-based materials would be an appropriate choice in composing and supporting imprinted sensing films, due to their unique properties such as well-defined tubular nano-sized structure, functional surface, appropriate chemical stability, strong electrocatalytic activity, and excellent biocompatibility. Therefore, electrochemically reduced graphene oxides (ERGOs) were used in electrochemistry as substrates for functionalization [35] and deposition of MIPs [36]. Various technological applications of reduced graphene oxide (RGO) are well summarized in a reviewing source [37]. The ERGO provides a more effective surface area to be imprinted in the presence of a template and monomer, increasing the number of recognition sites on the sensor surface [35].

In this study, we employed a new subsequent electrochemical-chemical procedure to establish the molecularly imprinted sensing film with an appropriate behavior in the assay of melamine. The procedure is based on the electropolymerization of PPy at ERGO/GCE which was followed by an oxidative treatment in alkaline-peroxide solution in an optimized mixed solvent medium. Using ERGO provides a more effective surface area to make possible the formation of a higher number of sensing sites in an ERGO-covered MIP film. The abovementioned steps are preceded by a critical adsorption step in solution of template, in which melamine could be gathered onto the surface of ERGO-GCE via hydrogen bond interactions between the functional groups of RGO and the nitrogen groups in melamine molecules. This event increases the number of recognition sites in the whole sensing film, and leads to higher sensitivity in response toward analyte. Here, in the process of the imprinting of polymer, melamine would be trapped into the PPy film through a donor-acceptor interaction, in which PPy plays the role of electron acceptor and melamine with its nitrogen-rich structure acts as a donor during the electropolymerization on ERGO/GCE [22, 24]. For the first time, this combined procedure was used to found a highly sensitive impedimetric melamine sensor.

Experimental

Reagents and materials

All chemicals were of analytical grade if it is not stated otherwise. Hydrogen peroxide, acetic acid, melamine, and other reagents were purchased from Merck. Pyrrole was from Sigma (Steinheim, Germany). Acetate buffer solution (ABS, 0.1 M, pH = 5.2) was used. The stock solution of 0.01 M melamine was produced by dissolving 0.126 g (1 mmol) of melamine in 100 ml of 1:5 (*v*/*v*) acetonitrile/water. The used milk sample in this work was obtained from a local supermarket. All electrochemical impedance spectroscopy (EIS) measurements were conducted in 5.0 mM $[Fe(CN)_6]^{4-/3-}$ + 0.1 M KCl. All aqueous solutions were prepared with double-distilled water.

Apparatus

Electrochemical measurements were performed using a μAutolab type III (Eco Chemie B.V.A) driven by GPES software (Eco Chemie) in conjunction with a conventional three-electrode system and a personal computer for data storage and processing. The conventional three-electrode system was applied with an Ag/AgCl (KCl_{sat}) electrode as a reference electrode and a platinum wire as the counter electrode. A glassy carbon electrode with a diameter of 2.0 mm coated with ERGO and modified with molecularly imprinted polymer (MIP/ERGO/GCE) was employed as the working electrode.

Fourier transformation infrared spectroscopy (FTIR) was recorded between 4000 and 450 cm^{-1} at a spectral resolution of 1 cm^{-1} on a Perkin-Elmer 1710 spectrophotometer using KBr pellets as reference at room temperature. Scanning electron microscope (SEM) images were achieved with scanning electron microanalyzer (TSCAN, Czech). A Metrohm (Model

780) pH meter with a combined glass pH electrode was used for pH measurements.

Electroanalytical measurements

The Faradaic impedance measurements in the solution of 5.0 mM of $[Fe(CN)_6]^{4-/3-}$ + 0.1 M KCl as a suitable redox probe were conducted over the frequency range of 100 kHz to 0.1 Hz at the particular open circuit potential (OCP) with an *ac* perturbation of 5 mV. The EIS spectra of the modified electrode follow a modified Randles' model in which the double-layer capacitance (C_{dl}) is replaced by the constant phase element (*CPE*). In this circuit, the solution resistance (R_s) arises from the finite conductance of the ions in bulk solution and this resistance is generally not affected by surface binding. The impedance results for a solid electrode/electrolyte interface often reveal a frequency dispersion that cannot be expressed by simple elements such as capacitance, resistance, and ideal Warburg impedance. The frequency dispersion is generally attributed to a "capacitance dispersion," which is expressed in terms of the *CPE* or *Q*. Different reasons for capacitance distribution have been reported in the literature as heterogeneities (fractal geometry and dilatational symmetry), electrode porosity or surface roughness, variation of coating composition, slow adsorption reactions, and current distribution [38, 39]. The Warburg impedance (*W*), only of physical significance in Faradaic EIS, represents the delay arising from diffusion of the electroactive species to the electrode. It is only appreciable at low frequencies and is affected by convection. R_{ct} is a manifestation of two effects: (i) the energy potential associated with the oxidation or reduction event at the electrode (i.e., overpotential) along with (ii) the energy barrier of the redox species reaching the electrode due to electrostatic repulsion or steric hindrance [40]. The sensor response was achieved from the change of charge transfer resistance (ΔR) at the interface of electrode/electrolyte in solution of $[Fe(CN)_6]^{4-/3-}$ before and after incubation of the sensor in the solution of different analyte concentrations.

Synthesis of ERGO

Before modification, the surface of GCE was polished with 0.05-μm alumina powders and was washed with distilled water for three times, subsequently. Then the electrode was ultrasonically cleaned with ethanol and distilled water for 5 min and dried at room temperature. Graphene oxide (GO) was synthesized using a modified Hummers and Offeman's method [41]. Typically, 0.5 g $NaNO_3$, 0.5 g graphite, and 23 ml H_2SO_4 were stirred together in an ice bath. In the following, 3 g $KMnO_4$ was slowly added to the mixture to oxidize the graphite intercalation compound. The mixed solution stirred at 35 °C water bath for about 2 h to a thick paste was obtained. Next, 40 ml water was slowly added and the solution was stirred for 30 min whereas the temperature was increased to 95 °C. After the addition of 100 mL water and 3 ml of H_2O_2 30%, the color of the solution altered from dark brown to yellow; H_2O_2 reacted with the excessive amount of $KMnO_4$. Finally, the obtained suspension was filtered, washed with 1 M HCl and double-distillated water, and vacuum-dried at 50 °C for 24 h to acquire GO.

For electrochemical conversion of GO to RGO, 2 μL of the homogeneous dispersed aqueous solution of GO (1 mg mL^{-1}) was casted on the bare GCE and dried under ambient conditions. The electrochemical reduction of surface-confined GO was performed by 20 successive CV scannings from − 1.8 to 0.0 V with sweep rate of 0.1 V s^{-1} in 0.1 M of PBS, pH 6.8 [42]. Finally, the ERGO/GCE was washed with double-distillated water and dried at room temperature.

Fabrication of the MIP-based sensor

The melamine sensor was constructed by electropolymerization of a molecularly imprinted film on the surface of ERGO/GCE using cyclic voltammetry over the potential range of − 0.4 to 1.0 V vs. Ag/AgCl. The process was conducted during five successive cycles in the solution of 0.1 M acetate buffer, pH 5.2, containing 10 mM of Py and 2.0 mM of melamine. In the following, the modified electrode was immersed in the mixture of 1:5 acetonitrile/water including 1% (*v*/*v*) H_2O_2 and 0.1 M NaOH for 5 min at room temperature. In the next step, the MIP/ERGO/GCE was immersed into a pH 5.2 ABS for 5 min to eliminate the excessive base from the imprinted polymer layer. For comparison, a non-imprinted polymer/ERGO/GCE (NIP/ERGO/GCE) was also fabricated following the same procedure, but in the absence of the template. A schematic of the construction procedure of the proposed sensor is shown in Scheme 1.

Results and discussion

Preparation and characterization of the electrodes

During electropolymerization of pyrrole in the presence of template, melamine was trapped in the polymer matrix. The mechanism of oxidation of pyrrole, as an irreversible process, was extensively studied [30]. The further chemical oxidation of the PPy film using hydrogen peroxide led to the improvement in conductivity and formation of cavity structures [34, 43]. In the inner wall of MIP cavities, the amine functional groups of melamine and pyrrole can interact through hydrogen bonding and π-π stacking. This interactions are directly affected by the orientation of interfacial chemical functions of cavities-template and the size conformity between imprinted cavity and template [43]. As a result, after the leaching

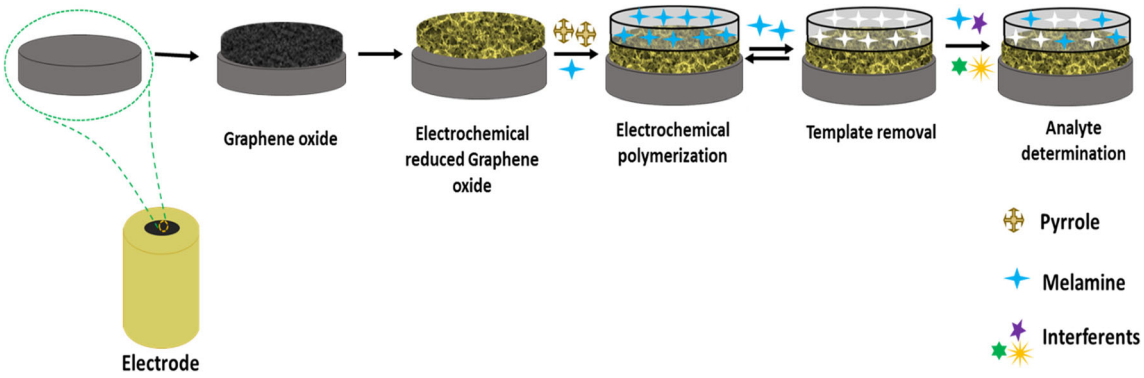

Scheme 1 Schematic of sensor preparation

process, the specific cavities toward template could be constructed.

As noted above, the electropolymerized film was fabricated on ERGO/GCE with five successive cycles in the buffer solution containing monomer and template. In detail, in the first cycle, an irreversible oxidation peak at 0.93 V emerged along with the anodic sweeping that was ascribed to the formation of amino cation radical (Fig. 1) [44]. In the next scans, the current of the anodic peak was drastically decreased, indicating that the polymeric film was deposited on the electrode surface. In other words, the decrease of the peak current by raising the scan number is ascribed to the continual formation of polymer films which hinders the Py monomer's further access to the electrode surface [40, 45, 46].

It should be noted that conductivity of the electrodeposited PPy depends on the condition of the electropolymerizaton setup, as in acidic medium a more conductive PPy film could be formed, and therefore, during electropolymerization the peak-current gradually increased [47, 48] whiles in neutral medium, around pH 6–7, the conductivity of PPy is lower [40]. Inspired by some similar PPy-based MIP research works [40, 45], and because under this condition melamine can be trapped in polymer without itself being polymerized, we therefore selected the neutral medium for electropolymerization (pH = 6), in which in the next step melamine would be easily extracted from the polymer backbone [22]. Such descending behavior was also reported for other monomers aminothiophenol [49] and *o*-hydroxyphenol [50].

After the electropolymerization step, the modified electrode was immersed in the solution of 1% H_2O_2 and 0.1 M of NaOH in the mixed solvents acetonitrile/water (1:5). In this step, two event could occur; in one of them, melamine was removed from cavities during facilitated release processes influenced by the strongly basic medium in the presence of acetonitrile as a swelling agent. Another is the further oxidation of the PPy film resulting in the formation of polarons and bipolarons that could increase the conductivity of the prepared film [34] (Scheme 2). A polaron is a charge associated with a lattice distortion that establishes a conjugate system to improve electron transfer properties along the electropolymerized film. Due to the fact that in higher pHs the positively charged electron holes, which are main charge carriers in PPy, are neutralized by the loss of protons from the polymer (Scheme 2), therefore, in the next step we need to treat leached MIP with ABS (pH = 6) to induce formation of polarons [34]. In conclusion, the proposed coupled electrochemical-chemical method includes the electropolymerization step for the preparation of a polymeric film, followed by two subsequent chemical steps that generate polarons and bipolarons through a proton-coupled electron transfer (PCET) reaction [51]. There was no distinct difference between the obtained cyclic voltammogram in the absence and presence of melamine, signifying the fact that melamine does not participated in the occurred redox event at ERGO/GCE.

Electrochemical verification of the *imprinted* sensor

Faradaic impedance spectroscopy that works based on evaluation of the electrode/electrolyte interface, in solution of a redox probe, was employed to monitor changes of charge transfer properties of the proposed sensor during different steps of the preparing and sensing procedures. Here, after incubation of MIP/ERGO/GCE in the melamine solution, the MIP cavities were occupied by melamine molecules and, consequently, the electron transfer capability of the redox probe was reduced. During this work, the change of signal was transduced by recording Faradaic impedance data, in the representation mode of the Nyquist plot, in solution of 5 mM $[Fe(CN)_6]^{4-/3-}$ + 0.1 M KCl as redox probe.

Figure 2 shows the influence of the stepwise fabrication procedure on the CVs, recorded in the solution of 5 mM $[Fe(CN)_6]^{4-/3-}$. The magnitude of redox peaks respective to the Fe(II)/Fe(III) couple on the bare GCE (Fig. 2a) was smaller than that on the higher electroactive surface area electrode, ERGO/GCE (Fig. 2b). It should be noted during electrochemical reduction of the graphene oxide that it could not

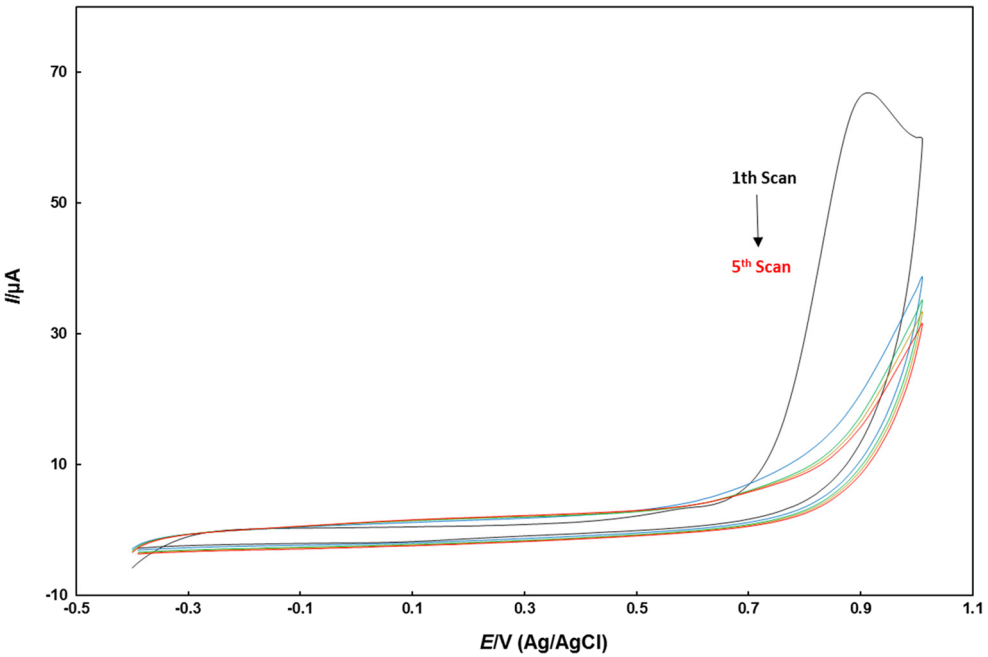

Fig. 1 Cyclic voltammograms for the electropolymerization of 10 mM PPy containing 2 mM melamine at ERGO/GCE in acetate buffer solution (pH 5.2). Scan rate, 50 mV s^{-1}; number of scans, 5

completely reduce and produce the ERGO with some part of oxygen-containing functional groups. The partially remained functional groups could increase the efficiency of electropolymerization of PPy via hydrogen-bonding [52].

After the electropolymerization of the polymer film on the ERGO/GCE surface, the current amplitude of redox peaks of the electrochemical probe decreases (Fig. 2c), confirming that the partly conductive film covered the nanostructure ERGO/GCE with higher effective surface area. After leaching the template by soaking the modified electrode in the solution of H_2O_2/NaOH, which was followed by incubation in the solution of ABS (pH = 5.2), the created polarons and the formed imprinted hollow cavities in the film that exposed a new path for redox probe molecules to arrive them on the under-layer platform led to an increase in the current amplitude of $[Fe(CN)_6]^{4-/3-}$ again (Fig. 2d). Figure 2e shows the MIP/ERGO/GCE, after being incubated in melamine solution, in which the redox peak declined, indicating that the binding sites in cavities of MIP are occupied by melamine.

Moreover, the EIS was employed to explore the features of the imprinted sensor. An ideal Nyquist plot shows a semicircle with the diameter corresponding to the charge transfer resistance (R_{ct}), attributed to the redox reaction performed at the interface of the electrode, and followed by a diagonal straight line corresponding to the impedance of the current due to diffusion from the solution to the interface (Warburg element,

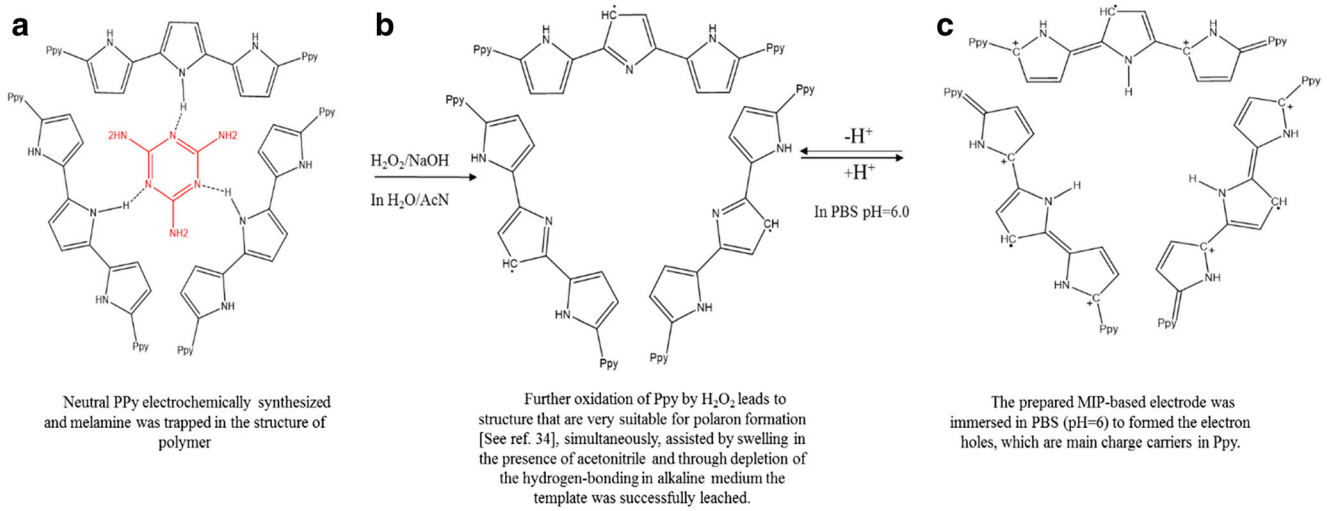

Scheme 2 **a** Electropolymerization of PPy and melamine trapping in the backbone of the polymer. **b** Leaching of melamine by acetonitrile as swelling agent, depletion of the hydrogen bonding in the alkaline medium and further oxidation of PPy in the presence of H_2O_2. **c** The increase in conductivity of the prepared MIP film by immersing in PBS (pH = 6)

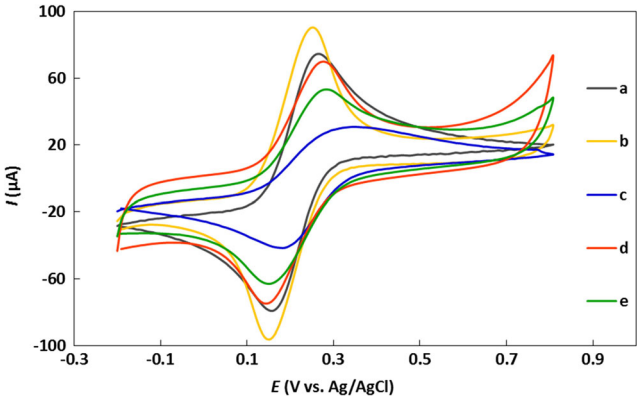

Fig. 2 Cyclic voltammograms in the solution of 5 mM $[Fe(CN)_6]^{4-/3-}$ + 0.1 M KCl at **a** bare GCE, **b** ERGO/GCE, **c** ERGO/GCE after electropolymerization, **d** MIP/ERGO/GCE, and **e** MIP/GCE after interaction with 80 nM melamine. Potential scan range, − 0.2 to 0.8 V; scan rate, 50 mV s^{-1}

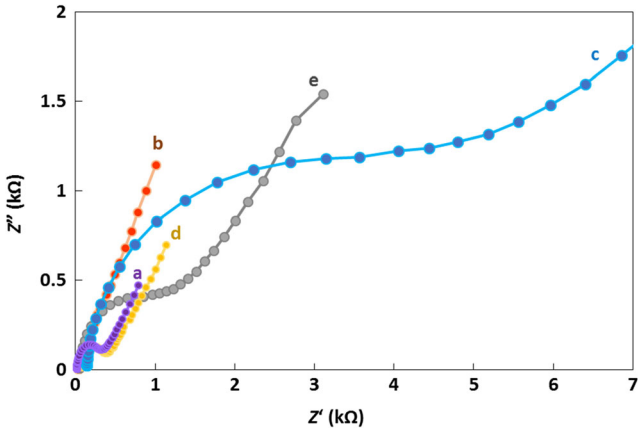

Fig. 3 The Nyquist plot obtained for **a** bare GCE, **b** ERGO/GCE, **c** ERGO/GCE after electropolymerization, **d** MIP/ERGO/GCE, and **e** MIP/ERGO/GCE after interaction with 80 nM melamine in the presence of a 1:1 mixture of 5.0 mM $[Fe(CN)_6]^{4-/3-}$ + 0.1 M KCl

W) [24, 40, 52]. Figure 3 represents the results of EIS in solution of 5.0 mM $[Fe(CN)_6]^{4-/3-}$ + 0.1 M KCl at bare GCE (a), ERGO/GCE (b), unleached MIP/ERGO/GCE (c), leached-MIP/ERGO/GCE (d), and MIP/ERGO/GCE after incubation in the solution of 80 nM of melamine (e). The ERGO/GCE exhibited an almost straight line, corresponding to a small heterogeneous charge transfer resistance at ERGO/GCE. After formation of the MIP film, the diameter of the semicircle was extensively increased (Fig. 3c). In comparison, at MIP/ERGO/GCE, the R_{ct} was evidently decreased due to the extraction of melamine from the imprinted polymer cavities and production of vacant sites in the polymer body (Fig. 3d). After incubation of the MIP/ERGO/GCE in melamine, the R_{ct} considerably increased, which could be attributed to the occupation of cavities in the polymer film (Fig. 3e). The redox peaks and R_{ct} of the non-imprinted electrode in the electrochemical probe show no notable change after treatment with melamine, showing that the surface of the electrode was completely covered by a partially conductive film.

FTIR was used to characterize the polymer separated from the electrode. The FTIR spectrum of separated PPy shown in Fig. 4 is in accordance to other reported literature [53, 54]. The characteristic peaks at 3412, 1559, 1369, and 1219 cm^{-1} in Fig. 4 confirm the presence of PPy. PPy, at 3412 cm^{-1}, shows a strong broad absorption band corresponding to the N-H stretching vibrations. The peaks at about 1369 and 1219 cm^{-1} reflects the C-N stretching vibration in the ring and CN in-plane deformation modes, respectively. The skeletal vibrations at 1559 cm^{-1} and the strong peak at 821 cm^{-1} characteristic of a five-membered aromatic ring were present [53].

The surface morphologies of ERGO/GCE and MIP/ERGO/GCE were examined with a scanning electronic microscope (SEM). The SEM image of ERGO (Fig. 5a) shows a typical flaky and crumpled graphite sheet structure. In the case of MIP/ERGO/GCE, a generally porous structure with the spongy sites signifies the successful formation of the MIP (Fig. 5b).

Optimization of analytical conditions

The parameters such as the concentration of template and monomer, electropolymerization cycles, applied potential, scan rate, extraction method, and incubation time control the thickness and physical stability of the polymer film formed at GCE/ERGO. Therefore, the effects of these parameters were considered by EIS and the optimized condition was employed, same as those expressed during experimental measurements. The change in charge transfer resistance (ΔR) was used before and after the sensor was dipped in the solution of 80 nM of melamine.

Effect of solvent and additives

Many methods can be employed to extract templates from the imprinting polymers. Extraction with a solvent or a mixture of solvents is one of the most common routes. Through the experiments, after some investigations, we found that the selected solvent can deeply influence the polymer layer and swell it, facilitating the extraction processes and extruding simply the trapped melamine template [22]. In this work, different ratios of acetonitrile/water and several NaOH concentrations in the absence and presence of H_2O_2 were used to remove the template molecule from cavities of the imprinted layer. The results showed that the solution containing 1:5 acetonitrile/water + 0.1 M NaOH and 1% (*v*/*v*) H_2O_2 provides the best performance in extracting melamine. The acetonitrile can induce swelling in the PPy film [30], and NaOH leads to the depletion of hydrogen-bonding between nitrogen groups in melamine and the PPy film at the inner interface of cavities and facilities the extrusion of melamine (Scheme 2). The addition of H_2O_2

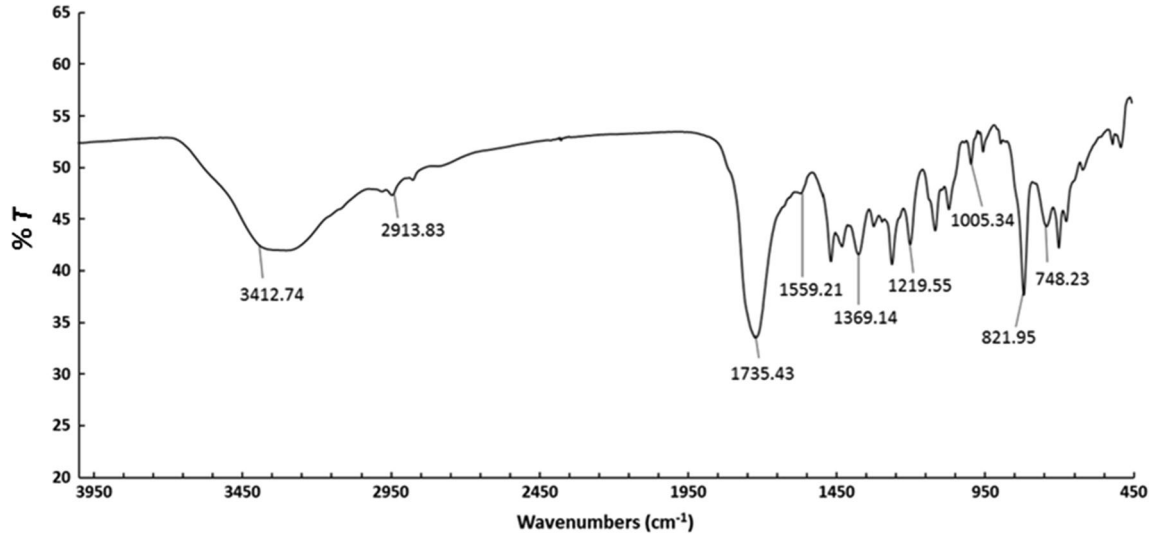

Fig. 4 FTIR spectrum of molecularly imprinted PPy films

in the solution oxidizes amine groups in interfacial cavity surfaces of the PPy film and causes formation of polaron and bipolaron in the bulk of the swelled polymer. Consequently, the latter event can accelerate the electron transfer along the partially conductive polymer film. To explore the role of this events, the process was repeated in solution without any oxidizing and alkaline agents, separately, which demonstrated that, in the absence of NaOH, the template partially leached and also in the absence of H_2O_2 the conductivity of polymer is slight, designating the critical roles of proposed additives in the leaching step.

Effect of monomer concentration

The concentration of monomer, during electropolymerization processes, has an important influence on the response of the proposed sensor. To explore the effect of monomer concentration on the analytical response of both MIP and NIP, electropolymerization was conducted in the solutions with constant concentration of melamine and varying pyrrole concentrations in the range of 4 to 14 mM and by cycling potential between − 0.4 V and + 1.0. Figure 6a shows the changes of charge transfer resistance (ΔR_{ct}) for MIP- and NIP-modified electrodes in the presence of 80 nM of melamine as a function of different concentrations of monomer. Contrary to GCE/ERGO/MIP which exhibited no significance change, the GCE/ERGO/MIP displayed a remarkable higher signal that altered and passed from a maximum around 10 mM of monomer concentration. This observed dependence should be proportional to the thickness of the deposited recognition layer, which is directly in accordance with the higher number of cavities in the electropolymerized layer. However, the passing R_{ct} from a peak designates this fact that an opposite balance is dominated between the number of cavities and thickness of film. As result, the optimum monomer concentration under these conditions was about 10 mM.

Effect of template concentration

In the further experiments, we considered the effect of template concentration, in the electropolymerization solution, on the response of the melamine sensor. Figure 6b shows the plot of ΔR_{ct} vs. the template concentration over the range of 0.5–3.0 mM. As it is shown, the response of the MIP/ERGO/GCE

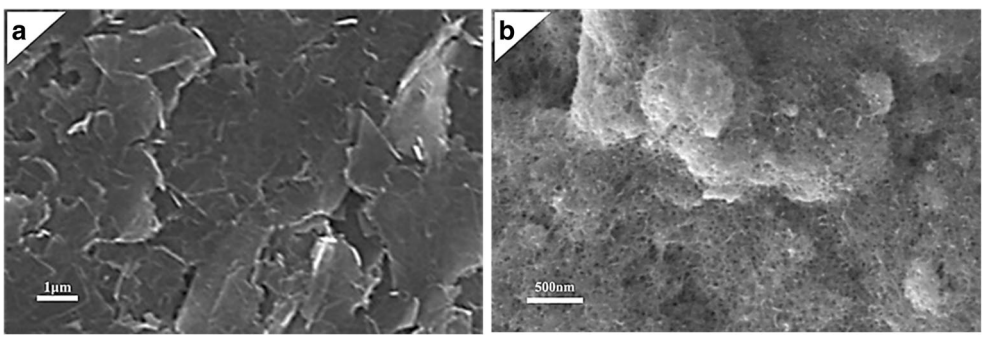

Fig. 5 SEM images of **a** ERGO and **b** imprinted PPy/ERGO films

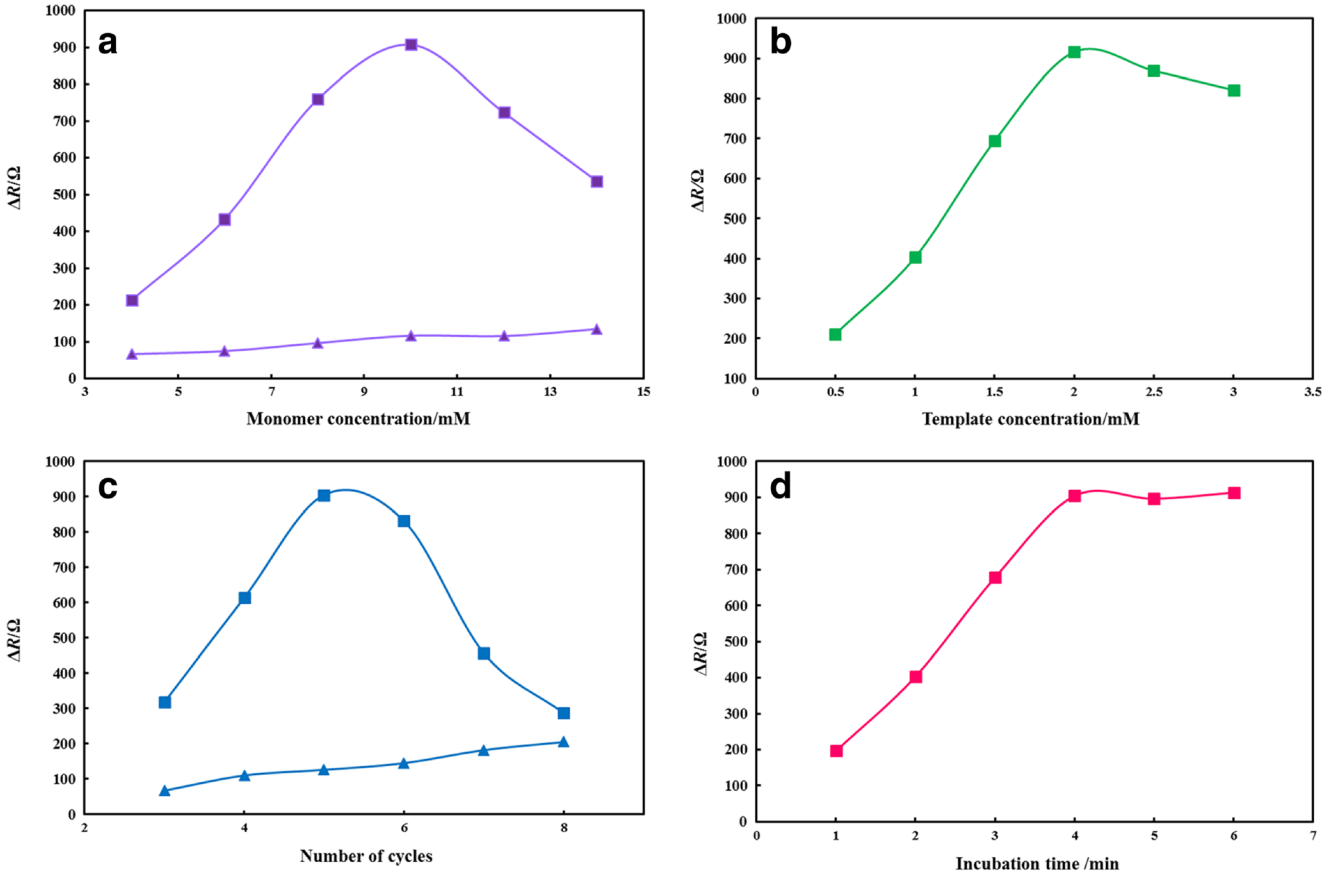

Fig. 6 **a** Effect of the monomer concentration during polymerization on the performance of MIP/ERGO/GCE (*filled square*) and NIP/ERGO/GCE (*filled triangle*). **b** Effect of the template concentration on MIP/ERGO/GCE response. **c** Effect of the number of cycles to MIP/ERGO/GCE (*filled square*) and NIP/ERGO/GCE response (*filled triangle*). **d** Effect of incubation time on MIP/ERGO/GCE response. The response was measured through EIS of a 1:1 mixture of 5.0 mM $[Fe(CN)_6]^{4-/3-}$ in 0.1 M KCl solution after immersion of the electrode in an 80 nM melamine solution for 4 min

to melamine rises with the increase of the template concentration between 0.5 and 2.0 mM and then displays a small decrease above 2.0 mM of the template. Therefore, the optimum template concentration was chosen as 2.0 mM.

Effect of number of cycles, range of applied potential, and scan rate

The number cycles during electropolymerization processes, considering the fact that it could directly affect the thickness and density of cavity sizes, could be important as a critical parameter and was found to impress the sensitivity and linearity of the sensor. The MIP electrode produced at the lower number of cycles exhibited a more favorable analytical performance (Fig. 6c). The higher number of cycles leads to more extensive electropolymerization and thicker sensing layer with larger R_{ct}, which may attenuate the capability of the sensing layer to read out the small change of charge transfer properties caused by the lower concentration of analyte. In addition, the higher number of cycle could yield a sensing film with less accessible imprinted sites. The highest ΔR_{ct} between the MIP and NIP electrodes for melamine was obtained by applying 5 cycles during electropolymerization. Thus, the optimum polymerization cycles were found to be five.

During this work, the potential range from − 0.4 to 1.0 V were used to carry out electropolymerization. The upper side potential was chosen as 1.0 V, because the anodic peak current was not observed at the lower positive potential was ca. 0.9 V. On the other side, when the positive potential of 1.1 V or higher values were employed, the oxidation peak became variable, demonstrating a suitable evidence for the formation of the overoxidaized polymer.

During electropolymerization, if the scan rate was lower, the electrodeposited PPy film would be thicker; it is known that the molecular template would be entrapped in the polymer firmly and it is difficult to be extracted. Contrarily, in extremely higher sweep rates, the formed film would be relatively porous and thin, which is not desirable for subsequent use [24]. Herein, in order to counteract the problem, we designed the scan rate as moderately high. The optimized scan rate was found to be 50 mV s^{-1}.

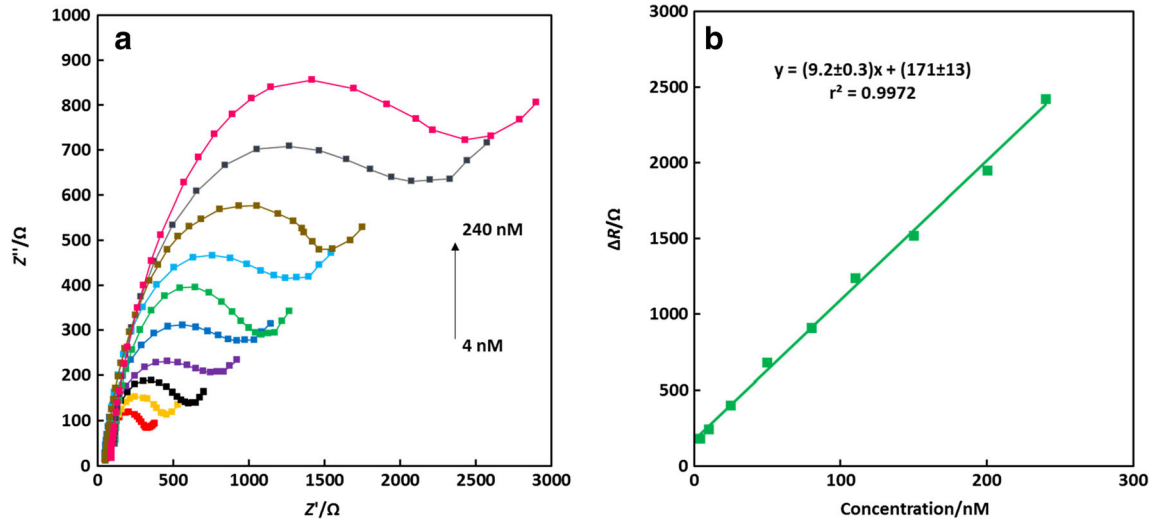

Fig. 7 **a** EIS of melamine (4 to 240 nM) on the MIP/ERGO/GCE and **b** calibration curve. The other conditions are the same as in Fig. 5

Effect of incubation time

The time of incubation for the sensor in the target solution has a critical importance for the establishment of new molecularly imprinted sensors. Thus, in order to determine the effect of the incubation time on the impedimetric detection of melamine, after the template molecules were removed from recognition sites of the modified electrode, it was incubated with stirring in the solution of 80 nM of melamine for different times in the range of 1 to 6 min, and the corresponding Nyquist plots were recorded in the redox probe (Fig. 6d). It was found that the electron transfer resistance increased rapidly up to 4 min and then leveled off, showing that the amount of absorbed melamine in the recognition sites of the PPy film increased as time was increased. After 4 min, the signal remained almost constant, implying that the adsorption equilibrium was reached under these experimental conditions. Consequently, an incubation time of 4 min was selected for all subsequent measurements.

Analytical performance

Calibration curve of the imprinted sensor

To evaluate analytical performance of the sensor under the optimal conditions, the Faradaic impedance signal in 5 mM $[Fe(CN)_6]^{4-/3-}$ + 0.1 M KCl, after incubation of the sensor in a series of the standard solutions of melamine, were recorded by the MIP/ERGO/GCE. As it can be seen from Fig. 7a, the impedance values (R_{ct}) increased with the increasing melamine concentrations, which can be interpreted by rebinding of melamine on the imprinted PPy layer, inhibiting the electron transfer of redox probes onto the electrode surface. The changes of electron transfer resistance ($\Delta R_{ct} = R_{ct2} - R_{ct1}$, where R_{ct1} and R_{ct2} are resistances obtained in the absence and presence of melamine, respectively) were plotted as a function of melamine concentration and show a linear range from 4.0 to 240 nM (Fig. 7b).

Table 1 Comparison of the fabricated sensor for melamine detection with other electrochemical methods

Methods	Linear range	Detection limit	References
Voltammetric sensor (MIP/GCE)	4.0 μM–0.45 mM	0.36 μM	[22]
Voltammetric sensor (oligonucleotides/Au)	0.039–3.3 μM	9.6 nm	[17]
MIP/CL	0.1–50 μg/mL	0.02 μg/mL	[57]
Potentiometric sensor	5.0 μM–10 mM	1.6 μM	[23]
LC	1–400 μg/mL	65 μg/g	[58]
HPLC-MS/MS	20–500 ng/mL	5.6 ng/mL	[59]
GC-MS/MS	0.004–1.6 mg/kg	0.002 mg/kg	[60]
Spectrophotometric method	1.26–10 μg/mL	0.2 μg/m	[61]
Acoustic chemosensor	5 nM–1 mM	5 nM	[21]
Impedimetric sensor (MIP/Au)	10 nM–50 μM	3 nM	[24]
Impedimetric sensor (MIP/ERGO/GCE)	4 nM–240 nM	0.83 nM	This work

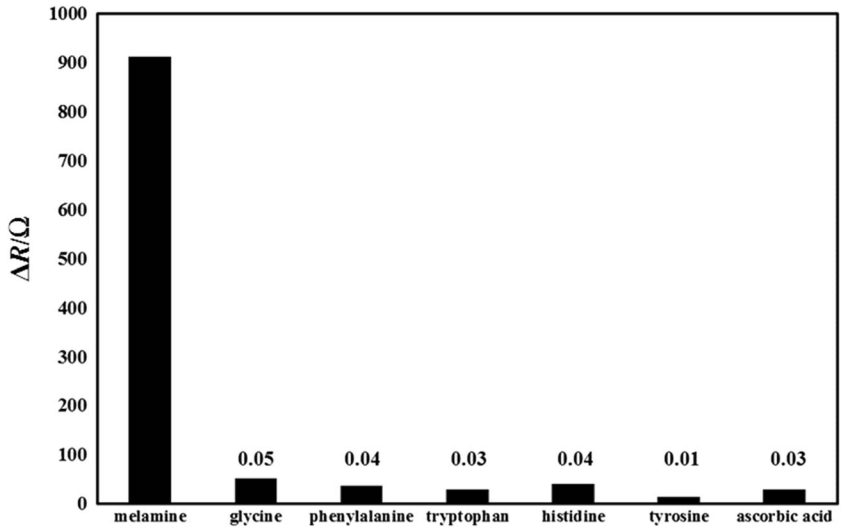

Fig. 8 Selective adsorption of the imprinted sensor to 80 nM melamine and 0.8 μM of each interference, respectively (the numbers on the columns are K = ΔRr/ΔRs)

The effect of indeterminate errors on the predicted slope and intercept as a useful demonstration of uncertainty was considered [55, 56]. The standard deviations of the slope and intercept were calculated to be 0.285 and 13.26, respectively. The linear regression equation is $\Delta R(\Omega) = (9.2 \pm 0.3)\ C$ (nM) + (171 ± 13) (r^2 = 0.9972). The detection limit was calculated to be 0.83 nM (based on the ratio of signal to noise, $S/N = 3$).

As demonstrated in Table 1, the results of the imprinted PPy/ERGO electrode for measuring melamine are compared with other published electrochemical methods. The results indicate that the proposed sensor presents a wider linear range and lower limit of detection compared to those reported for some other electrochemical methods.

The selectivity, in this work, was evaluated by comparing impedimetric responses of the proposed sensor in the presence of melamine with those obtained by some possible interfering substances like glycine, phenylalanine, tryptophan, histidine, tyrosine, and ascorbic acid. The selectivity coefficient is $K = \Delta R_r/\Delta R_s$, where ΔR_r is the equivalent relative charge transfer resistance change of 0.8 μM interfering material solution and ΔR_s is the relative charge transfer resistance change of sample solution containing 80 nM melamine. The response of the modified electrode toward melamine was higher than that for all nominated interferences (Fig. 8), which disclosed that the imprinted film has special recognition ability toward melamine molecules owing to the matched inner wall-functionalized cavities and the shape of melamine during the electropolymerization process, implying that the fabricated sensor might find further applications in the detection of melamine from complex samples without further separations.

Table 2 Determination of melamine in milk sample (n = 3)

Sample	Add (nM)	Found (nM)	Recovery (%)
Milk	0	0	–
	30	31.16	103.8 ± 3.1
	70	68.81	98.3 ± 1.2
	110	112.97	102.7 ± 1.8

Reproducibility and stability of the imprinted electrode

The reproducibility of the MIP/ERGO/GCE was evaluated in solution of 80 nM of melamine. The relative impedance change of melamine was determined with five electrodes which were produced under the same conditions. The response showed a relative standard deviation (RSD) of 4.1%, confirming that the results are reproducible. The repeatability of the sensor was also studied for 80 nM melamine, and the calculated RSD was about 3.1% (n = 5). The original response of the electrode retained 84.68%, when the electrode was kept in air for 30 days at room temperature. These results confirm that the electrode has acceptable reproducibility and stability.

Real sample analysis

To examine the applicability of the proposed MIP sensor, it was utilized to determine melamine in liquid milk bought from supermarkets. Because the existing milk in the market was free of melamine, the samples were directly spiked by certain amounts of melamine standard solution. The RSD of the results acquired by the proposed sensor ranged from 1.2 to 3.1%, and the recovery ranged from 98.3 to 103.8% (Table 2), suggesting that impedimetric determination of melamine using melamine-imprinted PPy/ERGO/GCE was effective and sensitive. Moreover, the obtained results demonstrated that the proposed method can be successfully used in the assay of melamine in milk samples.

Conclusion

In this work, an impedimetric sensor based on the melamine-imprinted polypyrrole deposited on ERGO/GCE was established. As mentioned above, the ERGO was utilized to amplify the electrochemical signal. A simple and inexpensive coupled electrochemical-chemical procedure was used for the construction of the sensing polymer. Using H_2O_2/NaOH solution in the extraction step, in addition to removal of melamine, conductivity was also increased through formation of positively charged species referred to as polaron and bipolaron. The designed electrochemical sensor exhibited good sensitivity, suitable selectivity, good reproducibility, and repeatability. The modified electrode provides a low detection limit and fast response for the detection of melamine. The proposed low-cost chemical sensor could find applications in the measurement of melamine in milk, exhibiting its capability as an accurate and fast sensor.

References

1. Parizanganeh A, Poorjafari N, Zamani A, Mohseni M (2015) Int J Environ Sci Technol 12:1003–1010
2. Kim B (2009) Analysis of melamine and cyanuric acid by liquid chromatography with diode array detection and tandem mass spectrometry. Electronic Theses and Dissertations Fogler Library. DigitalCommons@UMaine, The University of Maine, Publication number 3364705.
3. Tracy M (2010) The mutability of melamine: a transductive account of a scandal (respond to this article at http://www. therai. org. uk/at/debate). Anthropol Today 26:4–8
4. Dalal RP, Goldfarb DS (2011) Melamine-related kidney stones and renal toxicity. Nat Rev Nephrol 7:267–274
5. Bretterbauer K, Schwarzinger C (2012) Melamine derivatives—a review on synthesis and application. Curr Org Synth 9:342–356
6. Yokley RA, Mayer LC, Rezaaiyan R, Manuli ME, Cheung MW (2000) Analytical method for the determination of cyromazine and melamine residues in soil using LC-UV and GC-MSD. J Agric Food Chem 48:3352–3358
7. Zhu X, Wang S, Liu Q, Xu Q, Xu S, Chen H (2009) Determination of residues of cyromazine and its metabolite, melamine, in animal-derived food by gas chromatography−mass spectrometry with derivatization. J Agric Food Chem 57:11075–11080
8. Mauer LJ, Chernyshova AA, Hiatt A, Deering A, Davis R (2009) Melamine detection in infant formula powder using near-and mid-infrared spectroscopy. J Agric Food Chem 57:3974–3980
9. Yang S et al (2009) Detection of melamine in milk products by surface desorption atmospheric pressure chemical ionization mass spectrometry. Anal Chem 81:2426–2436
10. Lachenmeier DW, Humpfer E, Fang F, Schütz B, Dvortsak P, Sproll C, Spraul M (2009) NMR-spectroscopy for nontargeted screening and simultaneous quantification of health-relevant compounds in foods: the example of melamine. J Agric Food Chem 57:7194–7199
11. Chen Z, Yan X (2009) Simultaneous determination of melamine and 5-hydroxymethylfurfural in milk by capillary electrophoresis with diode array detection. J Agric Food Chem 57:8742–8747
12. Guo Z, Gai P, Hao T, Wang S, Wei D, Gan N (2011) Determination of melamine in dairy products by an electrochemiluminescent method combined with solid-phase extraction. Talanta 83:1736–1741
13. Wang Z, Chen D, Gao X, Song Z (2009) Subpicogram determination of melamine in milk products using a luminol− myoglobin chemiluminescence system. J Agric Food Chem 57:3464–3469
14. Tittlemier S (2010) Methods for the analysis of melamine and related compounds in foods: a review. Food Addit Contam 27:129–145
15. Han C, Li H (2010) Visual detection of melamine in infant formula at 0.1 ppm level based on silver nanoparticles. Analyst 135:583–588
16. Li L, Li B, Cheng D, Mao L (2010) Visual detection of melamine in raw milk using gold nanoparticles as colorimetric probe. Food Chem 122:895–900
17. Cao Q, Zhao H, Zeng L, Wang J, Wang R, Qiu X, He Y (2009) Electrochemical determination of melamine using oligonucleotides modified gold electrodes. Talanta 80:484–488
18. Cao Q, Zhao H, He Y, Ding N, Wang J (2010) Electrochemical sensing of melamine with 3, 4-dihydroxyphenylacetic acid as recognition element. Anal Chim Acta 675:24–28
19. Zhu H, Zhang S, Li M, Shao Y, Zhu Z (2010) Electrochemical sensor for melamine based on its copper complex. Chem Commun 46:2259–2261
20. Guan-Ping J, Bo Y, Zhen-Xin C, Xiu-Yu C, Ming Z, Chang Z (2011) Electrochemical behaviors and determination of melamine in neutral and acid aqueous media. J Solid State Electrochem 15:2653–2659
21. Pietrzyk A, Kutner W, Chitta R, Zandler ME, D'Souza F, Sannicolo F, Mussini PR (2009) Melamine acoustic chemosensor based on molecularly imprinted polymer film. Anal Chem 81:10061–10070
22. Liu YT et al (2011) Electrochemical sensor based on a poly (para-aminobenzoic acid) film modified glassy carbon electrode for the determination of melamine in milk. Electrochim Acta 56:4595–4602
23. Liang R, Zhang R, Qin W (2009) Potentiometric sensor based on molecularly imprinted polymer for determination of melamine in milk. Sensors Actuators B Chem 141:544–550
24. Wu B, Wang Z, Zhao D, Lu X (2012) A novel molecularly imprinted impedimetric sensor for melamine determination. Talanta 101:374–381
25. Huynh T-P, Pieta P, D'Souza F, Kutner W (2013) Molecularly imprinted polymer for recognition of 5-fluorouracil by RNA-type nucleobase pairing. Anal Chem 85:8304–8312
26. Piletsky S, Piletskaya E, Sergeyeva T, Panasyuk T, El'Skaya A (1999) Molecularly imprinted self-assembled films with specificity to cholesterol. Sensors Actuators B Chem 60:216–220
27. Haupt K (2001) Molecularly imprinted polymers in analytical chemistry. Analyst 126:747–756
28. Özcan L, Şahin Y (2007) Determination of paracetamol based on electropolymerized-molecularly imprinted polypyrrole modified pencil graphite electrode. Sensors Actuators B Chem 127:362–369
29. Sharma PS, Pietrzyk-Le A, D'Souza F, Kutner W (2012) Electrochemically synthesized polymers in molecular imprinting for chemical sensing. Anal Bioanal Chem 402:3177–3204
30. Vernitskaya TV, Efimov ON (1997) Polypyrrole: a conducting polymer; its synthesis, properties and applications. Russ Chem Rev 66:443–457
31. Ratautaite V, Janssens SD, Haenen K, Nesládek M, Ramanaviciene A, Baleviciute I, Ramanavicius A (2014) Molecularly imprinted polypyrrole based impedimentric sensor for theophylline determination. Electrochim Acta 130:361–367
32. Deore B, CHEN Z, NAGAOKA T (1999) Overoxidized polypyrrole with dopant complementary cavities as a new molecularly imprinted polymer matrix. Anal Sci 15:827–828

33. Ozkorucuklu SP, Sahin Y, Alsancak G (2008) Voltammetric behaviour of sulfamethoxazole on electropolymerized-molecularly imprinted overoxidized polypyrrole. Sensors 8:8463–8478
34. Leonavicius K, Ramanaviciene A, Ramanavicius A (2011) Polymerization model for hydrogen peroxide initiated synthesis of polypyrrole nanoparticles. Langmuir 27:10970–10976
35. Kong L, Jiang X, Zeng Y, Zhou T, Shi G (2013) Molecularly imprinted sensor based on electropolmerized poly (o-phenylenediamine) membranes at reduced graphene oxide modified electrode for imidacloprid determination. Sensors Actuators B Chem 185:424–431
36. Zaidi SA, Shin JH (2014) Molecularly imprinted polymer electrochemical sensors based on synergistic effect of composites synthesized from graphene and other nanosystems. Int J Electrochem Sci 9:4598–4616
37. Thakur S, Karak N (2015) Alternative methods and nature-based reagents for the reduction of graphene oxide: a review. Carbon 94: 224–242
38. Jorcin J-B, Orazem ME, Pébère N, Tribollet B (2006) CPE analysis by local electrochemical impedance spectroscopy. Electrochim Acta 51:1473–1479
39. Shamsipur M, Taherpour AA, Pashabadi A (2016) Interrupting the flux of delocalized electrons on a dibenzo-18-crown-6-embedded graphite sheet and its relative counteraction in the presence of potassium ions. Analyst 141:4227-4234
40. Uygun ZO, Dilgin Y (2013) A novel impedimetric sensor based on molecularly imprinted polypyrrole modified pencil graphite electrode for trace level determination of chlorpyrifos. Sensors Actuators B Chem 188:78–84
41. Cote LJ, Kim F, Huang J (2008) Langmuir−Blodgett assembly of graphite oxide single layers. J Am Chem Soc 131:1043–1049
42. Guo H-L, Wang X-F, Qian Q-Y, Wang F-B, Xia X-H (2009) A green approach to the synthesis of graphene nanosheets. ACS Nano 3:2653–2659
43. Syritski V, Reut J, Menaker A, Gyurcsányi RE, Öpik A (2008) Electrosynthesized molecularly imprinted polypyrrole films for enantioselective recognition of l-aspartic acid. Electrochim Acta 53:2729–2736
44. Shamsipur M, Pashabadi A, Taherpour AA, Hemmateenejad B, Khosousi T, Parvin MH (2016) Synthesis and characterization of glucose-capped CdSe quantum dots. Electrochemical and computational studies of corresponding carbon-ionic liquid electrode for quantitative determination of minoxidil. J Electroanal Chem 778: 116–125
45. Gupta VK, Yola ML, Özaltın N, Atar N, Üstündağ Z, Uzun L (2013) Molecular imprinted polypyrrole modified glassy carbon electrode for the determination of tobramycin. Electrochim Acta 112:37–43
46. Schweiger B, Kim J, Kim YJ, Ulbricht M (2015) Electropolymerized molecularly imprinted polypyrrole film for sensing of clofibric acid. Sensors 15:4870–4889
47. Wolfart F, Dubal DP, Vidotti M, Holze R, Gómez-Romero P (2016) Electrochemical supercapacitive properties of polypyrrole thin films: influence of the electropolymerization methods. J Solid State Electrochem 20:901–910
48. Alshammary B, Walsh FC, Herrasti P, de Leon CP (2016) Electrodeposited conductive polymers for controlled drug release: polypyrrole. J Solid State Electrochem 20:839–859
49. Xie C, Li H, Li S, Wu J, Zhang Z (2009) Surface molecular self-assembly for organophosphate pesticide imprinting in electropolymerized poly (p-aminothiophenol) membranes on a gold nanoparticle modified glassy carbon electrode. Anal Chem 82:241–249
50. Li H, Xie C, Li S, Xu K (2012) Electropolymerized molecular imprinting on gold nanoparticle-carbon nanotube modified electrode for electrochemical detection of triazophos. Colloids Surf B Biointerfaces 89:175–181
51. Hwang J-H, Pyo M (2007) pH-induced mass and volume changes of perchlorate-doped polypyrrole. Synth Met 157:155–159
52. Yang J, Deng S, Lei J, Ju H, Gunasekaran S (2011) Electrochemical synthesis of reduced graphene sheet–AuPd alloy nanoparticle composites for enzymatic biosensing. Biosens Bioelectron 29:159–166
53. Wang Y, Sotzing GA, Weiss R (2008) Preparation of conductive polypyrrole/polyurethane composite foams by in situ polymerization of pyrrole. Chem Mater 20:2574–2582
54. Thombare J et al. (2013) Studies on electrochemically synthesized polypyrrole (Ppy) thin films for supercapacitor application. Conference in: Energy efficient technologies for sustainability (ICEETS), International Conference on. IEEE, 1064–1067
55. Harvey D (2000) Modern analytical chemistry, vol 381. McGraw-Hill, New York
56. Miller JC, Miller JN (1988) Statistics for analytical chemistry. John Wiley and Sons, New York
57. Yu J, Zhang C, Dai P, Ge S (2009) Highly selective molecular recognition and high throughput detection of melamine based on molecularly imprinted sol–gel film. Anal Chim Acta 651:209–214
58. Muñiz-Valencia R, Ceballos-Magaña SG, Rosales-Martinez D, Gonzalo-Lumbreras R, Santos-Montes A, Cubedo-Fernandez-Trapiella A, Izquierdo-Hornillos RC (2008) Method development and validation for melamine and its derivatives in rice concentrates by liquid chromatography. Application to animal feed samples. Anal Bioanal Chem 392:523–531
59. Wu Y-T et al (2009) Determination of melamine in rat plasma, liver, kidney, spleen, bladder and brain by liquid chromatography–tandem mass spectrometry. J Chromatogr 1216:7595–7601
60. Hong M et al (2009) Simultaneous determination of melamine, ammelide, ammeline, and cyanuric acid in milk and milk products by gas chromatography-tandem mass spectrometry. Biomed Environ Sci 22:87–94
61. Rima J, Abourida M, Xu T, Cho IK, Kyriacos S (2009) New spectrophotometric method for the quantitative determination of melamine using Mannich reaction. J Food Compost Anal 22:689–693